

Raman study of crystal-field–phonon coupling in $\text{NdBa}_2\text{Cu}_3\text{O}_{7-\delta}$ in a magnetic field

T. Ruf, E. T. Heyen, and M. Cardona

Max-Planck-Institut für Festkörperforschung, Heisenbergstrasse 1, D-7000 Stuttgart 80, Federal Republic of Germany

J. Mesot and A. Furrer

Laboratorium für Neutronenstreuung, Eidgenössische Technische Hochschule Zürich und Paul-Scherrer-Institut, CH-5232 Villigen PSI, Switzerland

(Received 22 June 1992)

We study the influence of high magnetic fields on the coupled phonon–crystal-field excitation in the high-temperature superconductor $\text{NdBa}_2\text{Cu}_3\text{O}_{7-\delta}$ by Raman scattering. With wave functions obtained from inelastic neutron scattering, the Zeeman splitting of the Kramers degenerate crystal-field ground state is evaluated for magnetic fields along the main crystallographic axes. The twofold degeneracy of that excitation, which at zero field was found to couple with a phonon of the same symmetry, is lifted at finite fields. This is used to tune the energy of the crystal-field excitation with respect to that of the phonon. In Raman spectra for magnetic fields up to 16 T we observe broadenings, frequency shifts, and relative intensity changes for the lines of the zero-field doublet. This behavior is in agreement with theoretical predictions for the Zeeman splitting of the crystal-field excitation and the varying phonon content of the coupled wave functions.

I. INTRODUCTION

In recent Raman^{1,2} and inelastic neutron-scattering experiments³ the origin of a temperature-dependent double peak structure at the energy of the O(2)-O(3) out-of-phase vibration of the copper-oxygen planes in the high-temperature superconductor $\text{NdBa}_2\text{Cu}_3\text{O}_{7-\delta}$ was clarified. It was demonstrated that the doublet originates in a coupling of that phonon with a crystal-field excitation of the Nd^{3+} ions, which has the same symmetry and some energy close by. Convincing evidence for this explanation comes from the fact that the values for the unperturbed energies of phonon, crystal-field excitation and coupling constant obtained by the two methods are essentially the same. Raman scattering and inelastic neutron experiments were found to shed light on complementary aspects of the problem: The phonon content of the coupled wave functions is reflected in the Raman spectra, whereas in the geometry used neutrons are most sensitive to the admixtures of crystal-field excitations.²

The change in the coupling between phonon and crystal-field excitation was studied further by Raman experiments on samples where oxygen ^{16}O had been replaced by the ^{18}O isotope.² The resulting changes in the coupled excitation could be described solely by lowering the phonon frequency by a factor of $\sqrt{16/18}$, i.e., by taking the effect of isotopic substitution on the phonon into account. It appeared as a further challenge of the model developed to also change the energy of the crystal-field excitation with respect to that of the phonon. This can be achieved by applying a magnetic field, which even provides the possibility of continuously tuning the parameter of interest.

Relative intensities and energies of the crystal-field transitions of $\text{NdBa}_2\text{Cu}_3\text{O}_{7-\delta}$ found by inelastic neutron scattering were used to determine a set of crystal-field

parameters for Nd^{3+} ions in that environment.^{3,4} The Zeeman splitting of the crystal-field ground state appears as a sensitive test of the quality of the wave functions, which diagonalize the crystal-field Hamiltonian obtained in that way. Raman scattering emerges as the technique of choice in this case, since changes in the crystal-field energies can be observed via their coupling to a particular phonon. Also, the higher-energy resolution achieved with Raman as compared to inelastic neutron scattering is advantageous when small changes in the crystal electric field (CEF) levels are being studied.

In this paper we present a study along these lines. In Sec. II theoretical predictions for the Zeeman splitting of the crystal-field levels of $\text{NdBa}_2\text{Cu}_3\text{O}_{7-\delta}$ and the magnetic-field dependence of their coupling to the phonon are derived. In Sec. III we describe the experimental procedure. The results are presented in Sec. IV. A discussion of the experimental findings in relation to theoretical predictions is given in Sec. V and conclusions are drawn in Sec. VI.

II. THEORY

The ground state of the $4f^3$ electron configuration in Nd^{3+} is $^4I_{9/2}$. By spin-orbit coupling, the angular momentum of $L = 6$ and the spin $S = \frac{3}{2}$ combine to a total angular momentum of $J = \frac{9}{2}$. In the environment of a CEF of approximately D_{4h} tetragonal symmetry, such as in $\text{NdBa}_2\text{Cu}_3\text{O}_{7-\delta}$, the tenfold degenerate $^4I_{9/2}$ multiplet is split into five doublets, which retain the twofold Kramers degeneracy required for electron configurations with an odd number of electrons.^{2,5} The energies of these levels were determined by inelastic neutron scattering as 0, 97, 164, 304, and 932 cm^{-1} .^{3,4,6} A symmetry classification showed them to transform like the M_6^- , M_7^- ,

M_6^- , M_7^- , and M_6^- irreducible representations of the D_{4h} point group, written in the order of increasing energies.²

A crystal-field excitation and a phonon can couple to each other when they have the same symmetry. The bound state resulting from this interaction was investigated experimentally with Raman scattering in CeAl_2 ,⁷ where it manifests itself in a doublet structure with a pronounced temperature dependence. Magnetic-field effects on phonons, such as the splitting of doubly degenerate modes, due to this magneto-elastic coupling, have also been studied intensively on various other rare-earth compounds.⁸ Theoretical models were developed, which ascribe these observations to changes in the phonon content of the admixed wave functions and to relative changes in the energies and population factors of the excitations involved.^{2,9,10} The symmetry of a crystal-field excitation is given by the direct product of the irreducible representations of the contributing CEF levels. For the M_6^- and M_7^- levels of the $\text{NdBa}_2\text{Cu}_3\text{O}_{7-\delta}$ ground state in D_{4h} the following products are obtained:²

$$M_6^- * M_6^- = M_7^- * M_7^- = A_{1g} + A_{2g} + E_g, \quad (1)$$

$$M_6^- * M_7^- = M_7^- * M_6^- = B_{1g} + B_{2g} + E_g.$$

Therefore the O(2)-O(3) out-of-phase vibration of the copper-oxygen planes in $\text{NdBa}_2\text{Cu}_3\text{O}_{7-\delta}$, which has B_{1g} symmetry and an energy $\hbar\Omega_{\text{phonon}}$ around 308 cm^{-1} can interact with a CEF excitation such as the one between the ground state (M_6^-) and the level at $\hbar\Omega_{\text{CEF}}=304 \text{ cm}^{-1}$ (M_7^-).² It was found that a simple two-level model for the coupling between the phonon and the CEF excitation gives an adequate description of the phenomenon at low temperatures, where population effects and the influence of other CEF excitations can be neglected.² The renormalized energies of the coupled excitations are given by

$$\hbar\omega_{\pm} = \frac{\hbar\Omega_{\text{phonon}} + \hbar\Omega_{\text{CEF}}}{2} \pm \sqrt{\frac{(\hbar\Omega_{\text{phonon}} - \hbar\Omega_{\text{CEF}})^2}{4} + V^2}. \quad (2)$$

We treat the change in symmetry due to a magnetic field in the actual orthorhombic point group D_{2h} of $\text{NdBa}_2\text{Cu}_3\text{O}_{7-\delta}$. There all CEF levels of the $^4I_{9/2}$ ground state belong to the M_6^- representation and the excitations have A_g symmetry.² Magnetic fields along the x , y , or z axes lower the point group from D_{2h} to C_{2h} and the symmetry of M_6^- is reduced to $\Gamma_3^- + \Gamma_4^-$.¹¹ The symmetry of the O(2)-O(3) out-of-phase phonon is Γ_1^+ in C_{2h} . Taking the direct products we find that only $\Gamma_3^- * \Gamma_3^-$ and $\Gamma_4^- * \Gamma_4^-$ excitations can couple with the phonon. A magnetic field splits each of the Kramers doublets into states related by time-inversion symmetry, one with Γ_3^- and one with Γ_4^- character. To determine the magnetic-field dependence of the CEF excitations the Zeeman splittings and the characters of the constituent CEF levels have to be known. In the quasitragonal approximation, which was used for the interpretation of Raman selection rules¹² in rare-earth high- T_c cuprates, a magnetic field perpendicular to the copper-oxygen planes reduces the D_{4h} point symmetry to C_{4h} . The symmetries

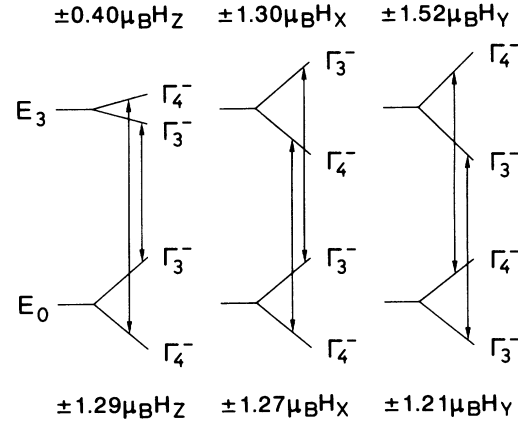


FIG. 1. Theoretical Zeeman splittings of the crystal-field levels E_0 and E_3 for magnetic fields along the three main axes of $\text{NdBa}_2\text{Cu}_3\text{O}_{7-\delta}$. The symmetries of the levels in the point group C_{2h} are indicated, and those crystal-field excitations between them which may couple to the O(2)-O(3) out-of-phase phonon are indicated by arrows.

of M_6^- and M_7^- are reduced to $\Gamma_5^- + \Gamma_6^-$ and $\Gamma_7^- + \Gamma_8^-$, the B_{1g} phonon belongs to the Γ_7^+ irreducible representation. The crystal-field excitations that couple to this phonon are given by the direct products $\Gamma_5^- * \Gamma_7^-$ and $\Gamma_6^- * \Gamma_8^-$. Magnetic fields parallel to the copper-oxygen planes reduce the D_{4h} point symmetry to C_{2h} and the analysis proceeds as above.

Wave functions for the CEF levels of interest were obtained from fitting a CEF Hamiltonian to the inelastic neutron-scattering data.^{3,4} It was found necessary to extend the set of basis functions beyond those of the ($J = \frac{9}{2}$) manifold. The positions and intensities of the lines in these spectra could be quantitatively described only when admixtures from the higher-lying multiplets $J = \frac{9}{2}, \frac{11}{2}, \frac{13}{2},$ and $\frac{15}{2}$ were allowed for via J mixing and intermediate coupling. Theoretical Zeeman splittings of the CEF levels E_0 (0 cm^{-1}) and E_3 (304 cm^{-1}) calculated with these wave functions are shown in Fig. 1 for various directions of the magnetic field. The changes in energy with magnetic field for each level are indicated as well as the irreducible representations according to which the states transform in point symmetry C_{2h} . Those crystal-field excitations, which by symmetry are allowed to couple to the O(2)-O(3) out-of-phase phonon, are connected by arrows. For each direction of the magnetic field there are two CEF excitations that have to be considered. Depending on the symmetries of the levels, the splitting of these excitations with field is either given by the sum or by the difference of the g factors of the individual levels. The g factors of the ground state are rather similar for all three directions with only a slight anisotropy for fields in the copper-oxygen planes. This is what one expects from the nearly tetragonal symmetry of $\text{NdBa}_2\text{Cu}_3\text{O}_{7-\delta}$. The g factors of the E_3 level differ by a factor of about 3.5 for fields perpendicular and parallel to the planes. Again a slight anisotropy is found for fields in the planes. Due to the symmetries of the Zeeman-split levels, the magnetic-field dependence of the total splitting

of the two CEF excitations, which couple to the phonon for each direction, is found to be $0.06\mu_B H_x$, $0.62\mu_B H_y$, and $3.38\mu_B H_z$. At a magnetic field of 16 T this corresponds to a separation in energy of 0.5 cm^{-1} , 4.6 cm^{-1} , and 25.2 cm^{-1} for these three directions.

Figure 2 summarizes the theoretically expected behavior of the coupled CEF-excitation phonon states in a magnetic field perpendicular to the copper-oxygen planes. The uncoupled excitations $\hbar\Omega_{\text{CEF}}(B)$ and the phonon energy $\hbar\Omega_{\text{phonon}}$ are indicated by the dashed lines in Fig. 2(a). The uncoupled energies at zero field were adjusted to values of $\hbar\Omega_{\text{phonon}} = (314.2 \pm 1.0)\text{ cm}^{-1}$ and $\hbar\Omega_{\text{CEF}} = (292.5 \pm 1.0)\text{ cm}^{-1}$ as found from Raman scattering. We used the coupling constant $V = (26.1 \pm 1.0)\text{ cm}^{-1}$, which was also determined from zero-field Raman data.

The energies of the coupled states were calculated with Eq. (2) and are given by the solid lines. The wave functions shown next to these lines indicate the symmetry of the constituent CEF levels. Diagonalization of the 2×2 problem, which led to Eq. (2) allows to calculate the admixed wave functions as a linear combination of phonon and CEF excitation. The phonon content, i.e., the square of the prefactor of the phonon part of the admixed wave functions can be regarded as a measure of the strength with which such a state contributes to the Raman spectrum.² Figure 2(b) plots the phonon contents for the four states of Fig. 2(a).

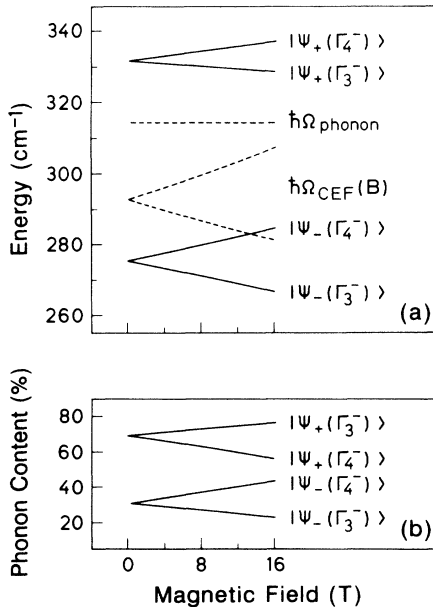


FIG. 2. Crystal-field excitation phonon coupling in $\text{NdBa}_2\text{Cu}_3\text{O}_{7-\delta}$. (a) Dashed lines indicate the uncoupled phonon $\hbar\Omega_{\text{phonon}}$ and CEF excitations $\hbar\Omega_{\text{CEF}}(B)$ vs magnetic field perpendicular to the copper-oxygen planes. Solid lines show the behavior of the coupled states calculated with Eq. (2). The symmetries of the constituent CEF levels for the C_{2h} point group are indicated in the labels of the admixed wave functions. (b) Phonon content of the coupled wave functions in percent.

III. EXPERIMENTAL PROCEDURE

The single crystal of $\text{NdBa}_2\text{Cu}_3\text{O}_{7-\delta}$ used in the present investigations was the same as that of Ref. 2. We studied the case where the direction of the magnetic field is perpendicular to the copper-oxygen planes of the crystal.

The sample was mounted in Faraday geometry in an optical exchange gas cryostat, which allowed it to be cooled down to about 10 K inside the bore of a 16-T superconducting magnet. Raman spectra were recorded in $z(x', y')\bar{z}$ geometry with a 0.85-m double monochromator using single-channel detection with a cooled photomultiplier and conventional photon counting electronics. The monochromator was set to a spectral width of 6.25 cm^{-1} . With such settings the influence of instrumental resolution on the observed linewidths could be kept below 0.5 cm^{-1} , while collection of most of the signal was still possible. The exciting photons had a wavelength of 514.5 nm and came from an Ar^+ -ion laser.

In order to avoid excess heating and possible damage to the sample, while still being able to collect enough signal for efficient single-channel detection, the laser power was kept between 20 and 30 mW with a spot diameter of about $200\text{ }\mu\text{m}$.¹³ Zero-field measurements at negligible laser power and varying temperature were compared to data taken at the lowest possible temperature for various laser powers. Comparison of the two sets of data showed that under the above conditions the actual sample temperature at which the experiments were performed was in the range of 50–60 K, even though the sample had been nominally cooled to liquid-helium temperature. At such temperatures the description of the CEF-excitation phonon coupling in terms of the 2×2 model outlined above is still a valid approximation.²

To facilitate the fitting of the data and the treatment of the scattering background, spectra were measured in the range of Stokes Raman shifts from $200\text{--}400\text{ cm}^{-1}$ with a step size of 0.5 cm^{-1} . The integration time was 10 s/step . With such parameters the experimental quantities peak position and line width could be determined with an accuracy of about $\pm 1\text{ cm}^{-1}$.

As the results will show, a clear separation of the splitting of the coupled CEF-excitation phonon states could not be observed, even at the highest available magnetic field. This is due to the rather large widths of the lines as compared to their Zeeman splitting. Nevertheless characteristic broadenings and frequency shifts of the features were found. To analyze the data we applied the following procedure. For all magnetic fields the experimental Raman spectra were fitted with two Lorentzians. From this we obtained values for the peak positions, effective widths and intensities of the lines. Keeping in mind that in a magnetic field each one of the coupled CEF-excitation phonon features should split into two lines, such as predicted in Fig. 2, we calculated theoretical Raman spectra with four Lorentzians using the experimental zero-field broadenings and the theoretical phonon contents of the wave functions as a measure of the expected Raman intensity. These spectra were then fitted with two Lorentzians, just like the experimental data, and the pa-

rameters obtained from these fits were compared to those obtained from fitting the real spectra.

IV. RESULTS

The effect of a magnetic field perpendicular to the copper-oxygen planes in $\text{NdBa}_2\text{Cu}_3\text{O}_{7-\delta}$ on the coupled CEF-excitation phonon states is shown in Fig. 3. As compared to the zero-field Raman spectrum the lower-energy structure shows an increase in its broadening from a half width at half maximum of $\Gamma_- = 8.2 \text{ cm}^{-1}$ to 14.3 cm^{-1} and an energy shift from $\hbar\omega_- = 275.9 \text{ cm}^{-1}$ to 281.5 cm^{-1} . The higher-energy feature remains nearly unaffected with widths of 9.8 cm^{-1} at zero field and 9.3 cm^{-1} at 16 T. Its Raman shift with 332.2 cm^{-1} (0 T) and 332.7 cm^{-1} (16 T) also only fluctuates within the experimental uncertainty. The relative intensity I_+/I_- of the higher- to the lower-energy peak, taken as the ratio of the areas of the fitted Lorentzians, is 2.4 at 0 T. We find it to be reduced to 1.3 at 16 T. The solid lines in Fig. 3 represent least-squares fits to the data using two Lorentzians. The horizontal bars indicate the effective full widths at half maximum of the fitted peaks; their positions are indicated by the arrows.

Figure 4 summarizes the results for the Raman shifts of the two peaks and their relative intensities vs magnetic field. The higher-energy structure remains almost constant over the range of fields up to 16 T with the tendency of a slight increase. The lower-energy structure shows a quadratic increase of its position with field. The position at 16 T is shifted by about 7 cm^{-1} from that at 0 T. The intensity ratio I_+/I_- decreases from an average of 2.3 at 0 T to 1.6 at 16 T. The changes in

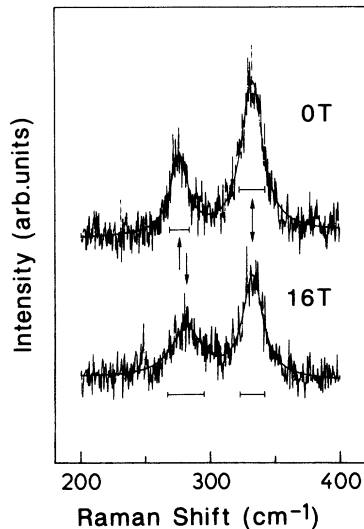


FIG. 3. Raman spectra of the coupled crystal-field excitation phonon states in $\text{NdBa}_2\text{Cu}_3\text{O}_{7-\delta}$ at magnetic fields of 0 and 16 T. With field the broadening of the lower-energy feature increases by almost a factor of 2 and its spectral position changes towards higher Raman shifts by 5.6 cm^{-1} . The higher-energy peak remains unaffected. Both spectra were fitted with two Lorentzians, which are indicated by solid lines.

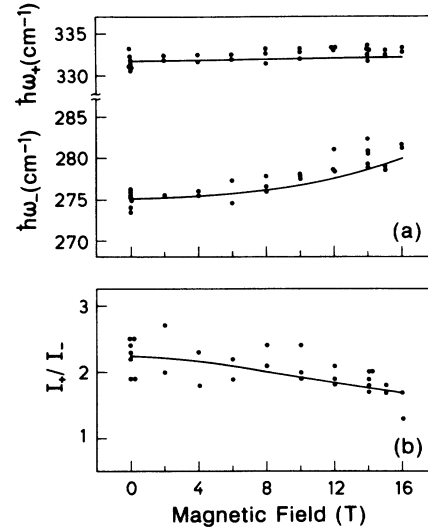


FIG. 4. (a) Positions of the coupled crystal-field excitation phonon states vs magnetic field for the higher $\hbar\omega_+$ and lower $\hbar\omega_-$ energy doublets. (b) The change in the relative intensities I_+/I_- of the two coupled features with magnetic field. Dots are experimental data, while solid lines show theoretical predictions.

the effective half widths at half maximum of the fitted Lorentzians are shown in Fig. 5. The higher-energy feature does not broaden within the experimental accuracy [Fig. 5(a)]. The lower-energy structure does exhibit a pronounced broadening with a quadratic dependence on the magnetic field [Fig. 5(b)]. The parameters obtained from fitting Lorentzian profiles to the data in both Figs. 4 and 5 are indicated by dots. Multiple dots at the same values of the magnetic field originate from repeated measurements and give an impression on the experimental accuracy.

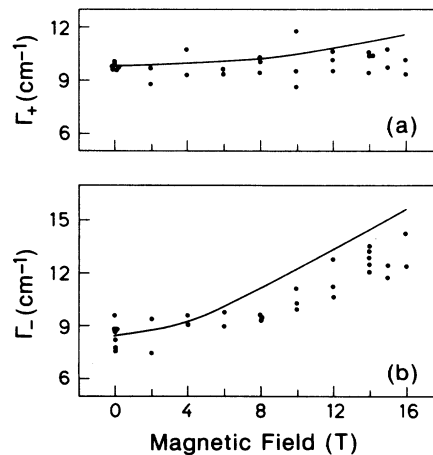


FIG. 5. Change in the effective widths of the (a) higher Γ_+ and (b) lower Γ_- energy coupled-state doublets in a magnetic field. Dots are experimental data, while solid lines show theoretical predictions.

V. DISCUSSION

The solid lines in Figs. 4 and 5 illustrate the predicted behavior of the experimental quantities according to the theory presented above. As mentioned before, theoretical values of the experimental parameters were obtained by calculating Raman spectra with four Lorentzians and then fitting them with two lines. This procedure was chosen due to the lack of clearly resolvable splittings of the coupled CEF-excitation phonon states. We find that there is good agreement between experimental parameters and theoretical values in all cases.

The magnetic-field dependence of the peak positions $\hbar\omega_+$ and $\hbar\omega_-$ in Fig. 4(a) can be understood from the theoretically predicted splittings of the coupled states and the changes in the phonon content of the wave functions that go along with it. For the lower-energy structure theory predicts a splitting of 17.5 cm^{-1} at 16 T (see Fig. 2). This is about the same as the full width at half maximum $2\Gamma_- = 17.0 \text{ cm}^{-1}$ of the line at 0 T. If the relative degree of admixture between phonon and CEF excitation in the coupled wave functions did not change with field, the energy position of one Lorentzian fitted to the field-dependent doublet would not change at all. From Fig. 2(b) we see, however, that the ratio of the phonon contents of the higher to the lower-energy states of the Zeeman-split doublet changes by a factor of 2 when the field increases up to 16 T. Therefore the Raman intensity around the lower-energy feature at zero field is going to be more and more dominated by the contribution from the higher-energy component of the split doublet in a magnetic field. This causes the energy of the unresolved doublet $\hbar\omega_-$ to be shifted towards higher energies. The expected splitting for the higher-energy doublet is 8.5 cm^{-1} at 16 T compared to a zero-field full linewidth of 19.6 cm^{-1} . The change in the admixture ratio amounts to only a factor of 1.4 at the highest field. However, in this case it is the scattering from the lower-energy level of the Zeeman-split doublet, which becomes enhanced. Also, for this doublet small quadratic corrections to the Zeeman energy, which originate in off-diagonal couplings between the admixed basis wave functions have to be considered. For the small splitting predicted in this case a slight shift of the mean value of the doublet's two peaks towards higher energies cannot be neglected. This shift can be seen in Fig. 2. It is the influence of these two factors acting in opposite directions, which causes the energy of one Lorentzian fitted to the split doublet $\hbar\omega_+$ to remain at the zero-field centered position up to much higher magnetic fields than in the case of $\hbar\omega_-$. In fact, almost no variation of $\hbar\omega_+$ is found nor predicted for fields up to 16 T.

The behavior of the effective line widths Γ_+ and Γ_- in Fig. 5 with magnetic field can be understood along the same lines. Fitting a single Lorentzian to a split doublet of two Lorentzians will at first not yield any dramatic change in the effective linewidth. For splittings small compared to the full linewidths of the individual peaks the fitted one Lorentzian adapts to the split lines in an optimum way such that its amplitude is increased but the width remains essentially unchanged. This leads to a

quadratic increase of the fitted linewidth with the splitting. At splittings larger than the full linewidths of the individual Lorentzians the width of one fitted Lorentzian increases linearly with the splitting. The behavior of Γ_+ and Γ_- in Fig. 5 illustrates these findings. Due to the larger splitting and the narrower linewidth the broadening of the lower-energy feature sets in at lower fields and the observed shifts are larger than for the higher-energy doublet.

The asymmetry of the uncoupled CEF excitations $\hbar\Omega_{\text{CEF}}(B)$ with respect to the undisturbed phonon $\hbar\Omega_{\text{phonon}}$ [see Fig. 2(a)] causes a change of the average phonon content for the higher- and lower-energy coupled doublets with magnetic field. As can be seen in Fig. 2(b), the average phonon content for the higher-energy Zeeman-split doublet decreases with increasing field, whereas that of the lower-energy doublet increases. This causes the ratio of the intensities I_+/I_- to decrease when a magnetic field is applied [see Fig. 4(b)].

When the neutron data are fitted with a crystal-field Hamiltonian set up for the ($J = \frac{9}{2}$) manifold only, the positions and relative intensities of the lines observed cannot be represented as well. The influence of higher lying crystal-field levels is expected to be important because the next multiplet (${}^4I_{11/2}$) is only 2000 cm^{-1} further up in energy.¹⁴ This separation is comparable to the total width of about 900 cm^{-1} of the $J = \frac{9}{2}$ ground state. We find that the most important effect of the higher contributions is to modify the admixture coefficients of the ($J = \frac{9}{2}$) states of the wave functions. Even though the contribution to the Zeeman splittings from the admixtures with J larger than $\frac{9}{2}$ is found to be negligible, the changes in the dominant coefficients themselves ($J = \frac{9}{2}$) cause rather pronounced differences. For the lowest Kramers doublet E_0 these effects lead to a change in the g factor by an order of magnitude and to a reversal of its sign. The splitting of the other crystal-field level of interest here, E_3 , is found to decrease by 60%, but its sign does not change when going from $J = \frac{9}{2}$ to J mixing and intermediate coupling wave functions. Considering $J = \frac{9}{2}$ wave functions only we find that the splittings of the E_0 and E_3 CEF levels subtract for the CEF excitations, which have the appropriate symmetry to couple to the phonon. Due to the smallness of the splitting for E_0 one would then essentially observe changes in the coupled CEF-excitation phonon states due to the splitting of E_3 . The behavior of the coupled states with magnetic field predicted by such wave functions is not in agreement with our experimental observations.

We have studied these effects for magnetic fields perpendicular to the copper-oxygen planes in $\text{NdBa}_2\text{Cu}_3\text{O}_{7-\delta}$. The agreement between theory and experiment gives confidence in the wave functions used to calculate the Zeeman splittings of the crystal-field levels. For in-plane magnetic fields the splittings of the relevant crystal-field excitations are thus anticipated to be rather small because of the unfavorable order in which states with the appropriate symmetries occur (see Fig. 1). With the small splittings calculated above we do not expect to observe a Zeeman effect on the crystal-field phonon coupling for magnetic fields parallel to the planes.

VI. CONCLUSIONS

We studied the effect of a magnetic field on the coupled crystal-field phonon states in single-crystal $\text{NdBa}_2\text{Cu}_3\text{O}_{7-\delta}$. The observed changes in energy positions, effective linewidths and intensity ratios are in accordance with the behavior predicted theoretically when the Zeeman splitting of the crystal-field excitations is calculated with wave functions obtained from fitting inelastic neutron scattering data to a crystal-field Hamiltonian, which takes J mixing and intermediate coupling into ac-

count. The splittings of the crystal-field states involved in the coupling are $\pm 1.29\mu_B H_z$ for the lowest level and $\pm 0.40\mu_B H_z$ for the level at 304 cm^{-1} .

ACKNOWLEDGMENTS

We would like to thank H. Hirt, M. Siemers, and P. Wurster for technical assistance and R. Wegerer for valuable discussions and a critical reading of the manuscript. Thanks are also due to G. Schaack for making us aware of Ref. 8.

¹E. T. Heyen, R. Wegerer, and M. Cardona, *Phys. Rev. Lett.* **67**, 144 (1991).

²E. T. Heyen, R. Wegerer, E. Schönherr, and M. Cardona, *Phys. Rev. B* **44**, 10 195 (1991).

³P. Allenspach, A. Furrer, P. Bruesch, and P. Untermaier, *Physica B* **156-157**, 864 (1989).

⁴P. Allenspach, Ph.D. thesis, Eidgenössische Technische Hochschule Zürich, 1991 (unpublished).

⁵K. R. Lea, M. J. M. Leask, and W. P. Wolf, *J. Phys. Chem. Solids* **23**, 1381 (1962).

⁶G. L. Goodman, C.-K. Loong, and L. Soderholm, *J. Phys. Condens. Matter* **3**, 49 (1991).

⁷G. Güntherodt, E. Zirngiebl, S. Blumenröder, A. Jayaraman, B. Batlogg, M. Croft, and E. Melczer, *J. Magn. Magn. Mater.* **47&48**, 315 (1985).

⁸K. Leiteritz and G. Schaack, *J. Raman Spectrosc.* **10**, 36

(1981); W. Dörfler and G. Schaack, *Z. Phys. B* **59**, 283 (1985); J. Kraus and G. Schaack, *ibid.* **74**, 259 (1989).

⁹P. Thalmeier and P. Fulde, *Phys. Rev. Lett.* **49**, 1588 (1982).

¹⁰P. Thalmeier, *J. Phys. C* **17**, 4153 (1984).

¹¹G. F. Koster, J. O. Dimmock, R. G. Wheeler, and H. Statz, in *Properties of the Thirty-Two Point Groups* (Massachusetts Institute of Technology Press, Cambridge, 1963).

¹²R. Liu, C. Thomsen, W. Kress, M. Cardona, B. Gegenheimer, F. W. de Wette, J. Prade, A. D. Kulkarni, and U. Schröder, *Phys. Rev. B* **37**, 7971 (1988).

¹³T. Ruf, C. Thomsen, R. Liu, and M. Cardona, *Phys. Rev. B* **38**, 11 985 (1988).

¹⁴K. N. R. Taylor and M. I. Darby, in *Physics of Rare Earth Solids* (Chapman and Hall Ltd., London, 1972).